Magazine of Civil Engineering

ISSN 2712-8172

journal homepage: http://engstroy.spbstu.ru/

Research article

UDC 624.014

DOI: 10.34910/MCE.112.15

Numerical modeling of basalt roll fire-protection for light steel thin-walled structures

***M.V. Gravit*[1], *I.I. Dmitriev*[2]** ✉

[1] *Peter the Great St. Petersburg Polytechnic University, St. Petersburg, Russia*
[2] *Graz University of Technology, Graz, Austria,*

✉ *i.i.dmitriev@yandex.ru*

Keywords: steel construction, thin walled structures, cold-formed steel, structural design, fire, fire safety, fire protection, fire design

Abstract. The authors investigate the fire-protective efficiency of a basalt roll material, which is used for light steel thin-walled structures. The values of fire-protective efficiency for the steel C-shaped profiles without fire protection made of basalt wool material MBOR-F were obtained in the experimental and numerical studies. This article presents the estimated dependence of the thickness of the fire-protective material MBOR F on the resistance to fire with regard to light steel thin-walled structures. The approximating functions are formed on the basis of the experimental data and presented as nomograms for heating of the steel structure. There was an absence of the samples' deformation and destruction of the fire-protective material during the fire tests. This allows us to conclude that the fire-protective efficiency of the light steel thin-walled structures increases by 2–4 times. Implementation of the study results will expand the scope of fire-protective materials for the light steel thin-walled structures, improve the quality of fire protection projects for buildings and constructions, and help ensure the fire safety of structural elements.

Acknowledgments: The authors are to the management of TIZOL JSC grateful for providing the results of the fire experiments, and also thank the specialists of Andromet LLC for providing technical and informational support in carrying out this work.

Citation: Gravit, M.V., Dmitriev, I.I. Numerical modeling of basalt roll fire-protection for light steel thin-walled structures. Magazine of Civil Engineering. 2022. 112(4). Article No. 11215. DOI: 10.34910/MCE.112.15

1. Introduction

Light gauge steel framing (LGSF) is widely used in low-rise constructions because of the wide architectural capabilities and excellent technical and economic qualities that allow for operation under dynamic conditions in a changeable market with maximum accuracy, flexibility, and efficiency. The advantages of light steel framing have already been appreciated in developed countries for several years, and buildings made from LGSF occupy a significant share of the construction market: in the UK – 20%, Sweden and Japan – 15%, Canada – 10% of total residential constructions. The share of LGSF in Russian low-rise construction is 0.5% – that is 30 times less than in developed countries [1,2].

The LGSF constructions have great perspectives in the design area [3, 4], however, low levels of fire resistance of unprotected thin-walled constructions inhibit the process of incorporating designs into construction. The fire resistance of thin-walled rods is actively discussed throughout the world, but, despite numerous investigations of these structures, this issue has not been fully studied and remains relevant. For the widespread introduction of light steel thin-walled structures into the civil engineering practice of public and residential constructions, it is necessary to conduct tests to determine the fire resistance of structures and to allow for the subsequent improvement of existing regulatory documents.

The fire protection of the building structures is an integral part of the general system to ensure fire safety and fire resistance of buildings and constructions [5,6]. The light steel framing has a short resistance period under fire loads, and because of that, it is not required by Russian fire safety standards. In some cases, these systems do not reach the minimum requirement of the safety conditions, and therefore the fire protection plays an important role in obtaining the required fire resistance of various configurations of LGSF constructions.

There are a small number of works concerning the fire resistance of LGSF, which include consideration of the regulatory framework in our country compared with the other ones. The conducted studies include those by Vatin and Garifullin [7–11], Gravit [12–15], Naser [16–18], Chen and Ye [19–23], Dias [24,25], Craveiro [26]. Researchers have also determined that cold-formed steel perforated beams can have higher fire resistance than the limit of 350 °C, according to Eurocode 3 [26 – 35]. Many studies on the behavior of thin-walled steel constructions were conducted not only for the standard fire mode, but also as numerical simulations of real fire scenarios.

Naser and Degtyareva reported the results of the fire tests on the steel beams made of galvanized C-shaped thermal profiles [16]. In these experiments the authors investigated the stress limits of the perforated beams as well as their temperature deformations. The result of this work was a nonlinear numerical model, developed by using the finite element analysis software ANSYS.

The fire test results of cold-formed steel columns of both the single and built-up section of 2xC-shaped profiles are presented in [26]. The temperature increment depended on the cross-sectional shape. Therefore, a C-shaped column with a section factor 400 m-1 and a column with built-up 2xC-shaped profile have reached the limit state for stability only after 8 minutes and 10 minutes respectively. Structures were under the temperature load in according to the standard fire curve. The critical temperature of profiles exceeded 500 °C. Numerical simulations using the Abacus software has also been conducted.

The fire resistances of the steel columns were evaluated by numerical simulations in [27], taking into account the various thicknesses of the fire protective coating made of the vermiculite plates. Three column options were considered: columns without fire protection, with protection of 20 mm thickness, and with 40 mm thicknesses. The temperature contour graphs and heating curves of the columns were obtained by taking into account the presence and absence of fire protection made of the vermiculite plates. Studies have shown that the steel columns covered by a fire-protective layer with 20 and 40 mm thickness and the unprotected steel column sustained a critical temperature of 500 °C after 82, 180 and 12 minutes, respectively.

The constructive method of the steel structures' protection with PYRO-SAFE AESTUVER T plates and the fire resistance limit of steel rod elements were considered in [28] to ensure the regulatory fire resistance requirements. This paper presents the calculated thermophysical characteristics of materials, based on which the fire resistance nomograms of the fire protected steel structures are calculated. For instance, both the steel construction with 2 mm profile thickness and the steel plate with 20 mm profile thickness sustained a critical temperature of 600 °C after 70 minutes (and 80 minutes for the steel with 3.4 mm profile thickness); the steel plate with 40 mm profile thickness sustained a critical temperature of 600 °C after 100 minutes.

Therefore, despite the fact that there are some researches into unprotected light steel structures and structures with different types of fire-protective materials (both structural and paintwork), this number of studies is insufficient, because the problem with underestimation of light steel framing is actual and the industry still has a need for new technologies and materials for fire protection.

The aim of this study was to evaluate the fire-protective efficiency of MBOR roll material based on basalt wool manufactured by TIZOL JSC (Russia) for LGSC structures. To achieve this goal, the following tasks were carried out:

1. The conduction of experimental studies of C-shaped profiles, including fire protection with MBOR rolled basalt material;

2. The modeling of the thermal effect on building structures (LGSC) in the ELCUT PC, including MBOR fire protection;

3. The creation of recommendations on the use of flame protective materials for structures (LGSC).

The results of fire tests allow us to evaluate the accuracy of both analytic and numerical (computer) modeling methods. The authors used the results of fire impact on light gauge steel structures, and carried out experiments in the testing laboratory of TIZOL JSC, for a comparative analysis.

The results of the numerical studies on the cold-formed steel galvanized profiles with fire protection by heat-insulating plates made of MBOR-F basalt wool are presented. Fire-protective efficiency and

behavior of LGSC profiles are determined according to experimental studies and using linear FE models developed in the ELCUT PC and verified according to fire tests.

2. Methods

2.1. Fire test method

The tests of LGSC profiles with fire protection made of heat-insulating basalt wool plates MBOR-F and PLAZAS adhesive composition are carried out in accordance to Russian Standard No. 53295-2009 [36] with four-sided heat exposure according to the standard temperature curve according to ISO 834 [37]. The method allows for the determination of the actual efficiency of the fire protection, which is equal to the time from the onset of the thermal effects on the prototype until the limit state of this sample. The critical state corresponds to the critical temperature of heating the section of the structure.

The equipment includes:

- a test furnace with a fuel supply and combustion system;

- devices for installing the sample in the furnace;

- systems for measuring and recording parameters according to [37].

There was a standard temperature mode characterized by the equation:

$$T - T_0 = 345 \lg(8t + 1) \quad (1)$$

where t is the time calculated from the start of the test, minutes;

T is the furnace temperature corresponding to time t, ℃;

T_0 is the temperature in the furnace before the start of the heat exposure (ambient temperature), °C;

The structural elements based on cold-formed steel galvanized profiles without taking into account the static load were investigated to determine the behavior of light steel thin-walled structures and to increase their fire resistance. As the test object, rod structures of a composite section made by Andrometa LLC from two C-shaped profiles connected by bolt fastening are adopted (technical specification: TC 1122-002-82866678-2013 "Cold-formed profiles from galvanized steel for construction):

- sample No. 1 - 2AC 150 × 75 × 16.8 × 1.6 mm;

- sample No. 2 - 2AC 380 × 125 × 29.9 × 3.5 mm.

The coating is designed as a single-layer sheathing basalt roll material. The MBOR material is a staple canvas of basalt super thin fibers, stitched with a knitting and stitching method and lined with aluminum foil on one side. The schemes of the test structures and the basic geometric characteristics of the profile are presented in Figure 1 and Figure 2.

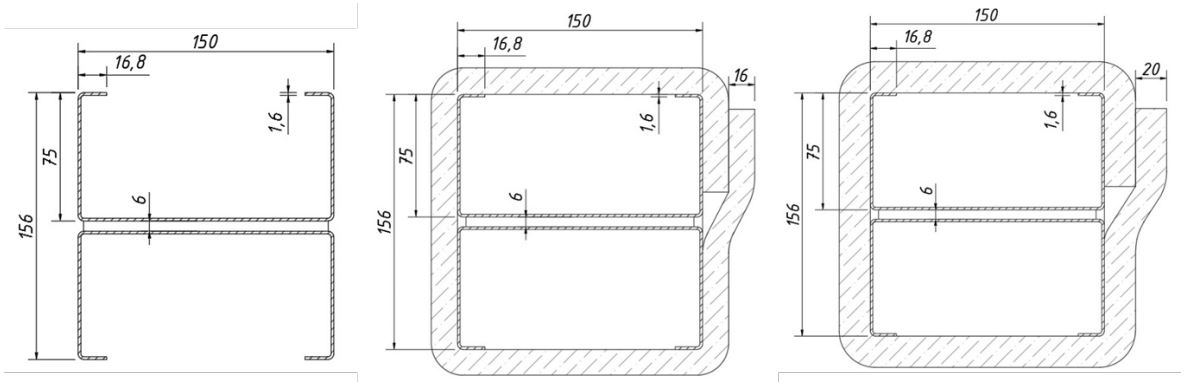

Figure 1. Test sample No. 1.

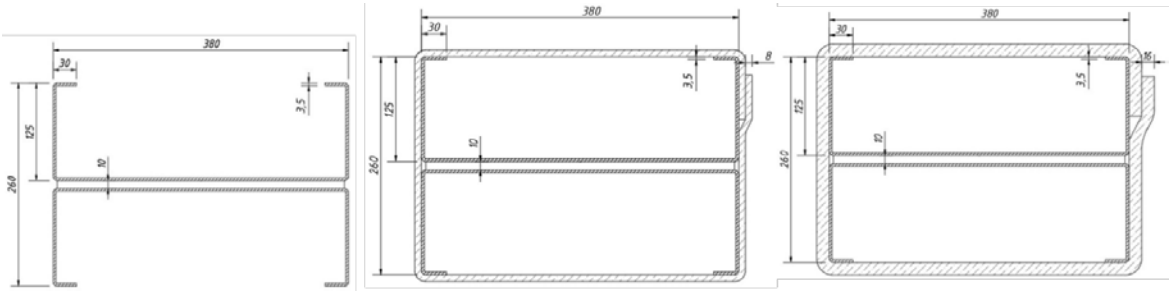

Figure 2. Test sample No. 2.

There were six test samples with a length of 1700 ± 10 mm. The concept of the reduced metal thickness, t_{red} , was used to compare metal structures. It is defined as the ratio of the cross-sectional area to its heated perimeter for each test sample by the formula (2):

$$t_{red} = \frac{S}{P} \tag{2}$$

where S is the cross-sectional area of the metal structure, mm^2,

P is the heated part of the structure perimeter, mm.

The reduced thicknesses of the steel of construction No. 1 and No. 2 according to the formula (2) are:

Sample 1, 150×150×1700 t_{red1} = 1.01 mm (section factor 990,1 m^{-1})

Sample 2, 250×380×1700 t_{red2} = 2.35 mm (section factor 423.7 m^{-1}).

The design of the furnace is shown in Figure 3. Temperature measurements of samples are controlled by thermocouples in the middle section on the inner surface. The method of attaching the thermocouples is shown in Figure 4.

Figure 3. Fire Test Furnace

Figure 4. Installation locations for thermocouples

The test samples (Fig. 5, 6) were exposed to a high-temperature environment in a test furnace during the experimental study until the time of reaching the set temperature (t = 700°C). The higher critical temperature was chosen in order to investigate the behavior of the fire protective material also under conditions exceeding the standard ones (when tested in accordance with GOST R 53295 [36] without load, the critical temperature is 500°C). A characteristic feature of all experiments is that when the object of study reaches its limit state, the fire exposure ceases.

Figure 5. Unprotected prototype No. 1 during and after the test.

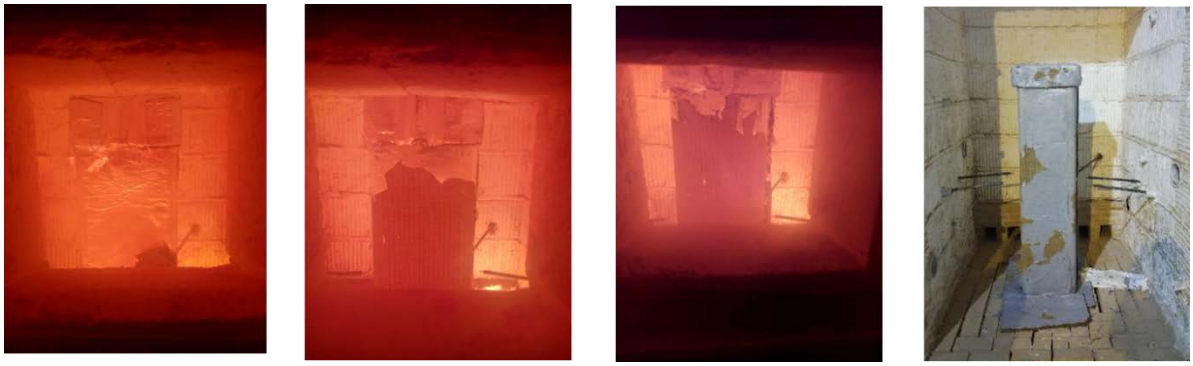

Figure 6. Prototype No. 2 protected by material MBOR-F during and after the test.

2.2. Modelling in ELCUT PC

Models of steel structures with and without fire protection developed in the ELCUT PC [38–41] were validated according to the fire tests. The two-dimensional model is calculated in the transient thermal conductivity module. Materials have isotropic properties. The heat source is distributed along the cross-sectional contour. The boundary conditions of the considered models correspond to the boundary conditions of the experimental method and belong to the first kind of model classification (the change in the temperature of the external environment is specified). The rise in ambient temperature follows the standard fire curve. The initial temperature is 20 °C. The sampling step of the model is equal to 1 mm. Iteration over temperature is equal to 60 s.

For all tested cross-sections the adopted convective heat transfer coefficient 25 W/m^{2}K used for ISO 834 fire curve for the fire test curves. The radiative heat flux was calculated using a steel (cold-formed steel with zinc coating) emissivity of 0.24 and 0.7 for the furnace electrical resistances (ε = 0.168). The Stefan-Boltzmann constant was 5.67×10-8 W/m^{2}K. The temperature distribution obtained from these numerical simulations will be used as input in the finite element structural models, considering a uniform temperature along the length of the column.

All structural calculations are performed by the finite element method based on the spatial finite element model shown in Figure 7. The properties of the elements are set in accordance with the real properties of steel and the geometric dimensions of the structures. The thermotechnical characteristics of the materials of the finite element model are presented in Figure 8 and Figure 9.

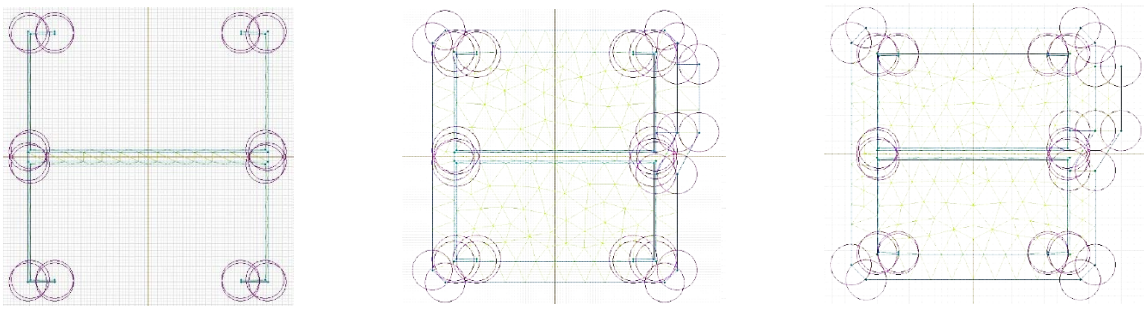

(a) Test 1 **(b) Test 2** **(c) Test 3**

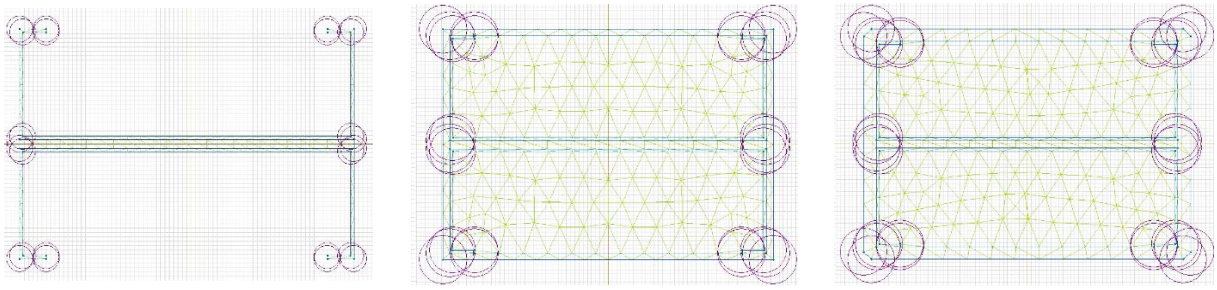

(d) Test 4 **(e) Test 5** **(f) Test 6**

Figure 7. Finite-element models of the design sections: a, b, c – sample No. 1; d, e, f – sample No. 2.

Strength characteristics of steel:

R_0 is an initial standard metal resistance, kg/cm²; and it is equal for steel C350 to $R_0 = 3500\text{kg/cm}^2$.

E_0 is the initial modulus of elasticity of the metal at normal temperature, kg/cm², $E_0 = 2{,}100{,}000\text{kg/cm}^2$.

The thermotechnical characteristics of materials are accepted on the basis of the document "Design of fire protection of load-bearing steel structures of multi-apartment residential buildings" [42]:

Steel density: $\gamma_{st} = 7850\text{kg/m}^3$.

The coefficient of thermal conductivity λ_t (W/m · K) varies according to the formula (3):

$$\lambda_t = A + Bt, \tag{3}$$

where A is the initial coefficient of thermal conductivity, (W m · K);

B is the coefficient of change in thermal conductivity during heating, (W/m · K);

t is the material heating temperature, K.

The heat capacity coefficient C_t (J/kg · K) varies according to the formula (4):

$$C_t = C + Dt, \tag{4}$$

where C is the initial heat capacity coefficient, (J/kg · K);

D is the coefficient of change in heat capacity during heating, (J / kg · K);

t is the material heating temperature, K.

The values of these coefficients for calculations in software systems are presented in Table 1.

Table 1. The coefficients of the thermal characteristics of materials.

№	Steel	Fire protective material MBOR F
A	78	0.032
B	-0.048	0.00029
C	310	850
D	0.48	0.45

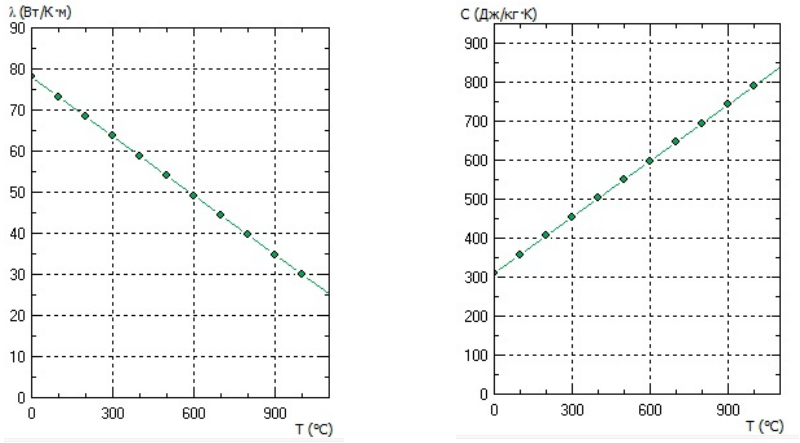

Figure 8. Changes of thermal conductivity and heat capacity of steel with heating temperature.

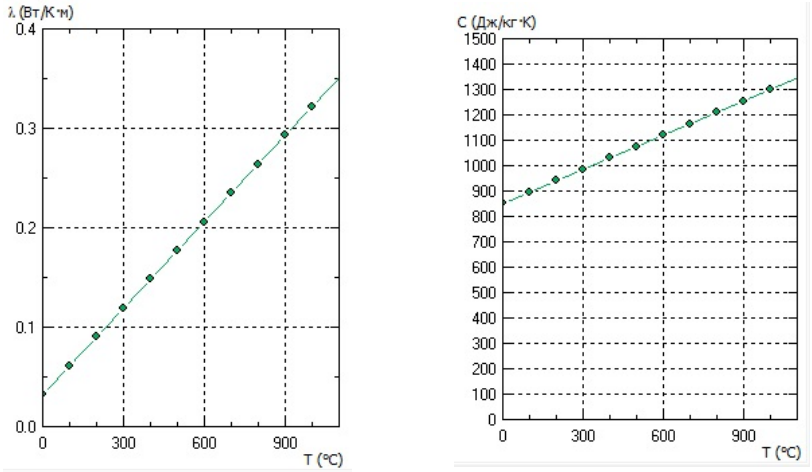

Figure 9. Changes of thermal conductivity and heat capacity of MBOR-F flame retardant material with heating temperature.

The system is uniformly heated by the external heat flow; the whole energy spends on the raising of temperature and the heating stops when the temperature at the external boundaries is equalized with the temperature of the external irradiating medium, which corresponds to a given temperature in the furnace.

3. Results and Discussion

3.1. Experiment Results

The experimental result of the sample is the time of onset of its ultimate state. The results of fire tests to achieve steel structures of critical temperature are shown in Table 2 (average value of thermocouples, Fig 10, 11).

Table 2. Fire Test Results.

t_{red} , mm	The time to reach the critical temperature of 700 ˚C (Temperature in the furnace, ˚C)			
	Unprotected	Thickness of the fire protective coating, mm		
		8	16	20
1.01	15:35 (743.1)	-	48:35 (899.3)	50:43 (912.2)
2.35	17:27 (759.0)	50:08 (904.4)	69:02 (969.3)	-
t_{red} , mm	The time to reach the critical temperature of 500 ˚C			
	Unprotected	Thickness of the fire protective coating, mm		
		8	16	20
1.01	4:57	-	33:35	37:43
2.35	9:15	37:08	48:02	-

3.1.1. Evaluation of the flame protective efficiency of basalt roll material

The time to reach of limit state for unprotected prototypes based on the temperature-time curves of the fire tests was 15 (sample No. 1) and 17 minutes (sample No. 2). However, if these samples are sheathed with MBOR-F basalt material, the time of fire exposure increases several times.

The fire resistance of the structure increased by three times for steel sample No. 1 with the MBOR-16F and MBOR-20F materials. There are similar results for sample No. 2. Figure 10 and Figure 11 show the data of experiments conducted at different thicknesses of the MBOR-F material for structures with reduced metal thicknesses of t_{red1} = 1.01 mm and t_{red2} = 2.35 mm.

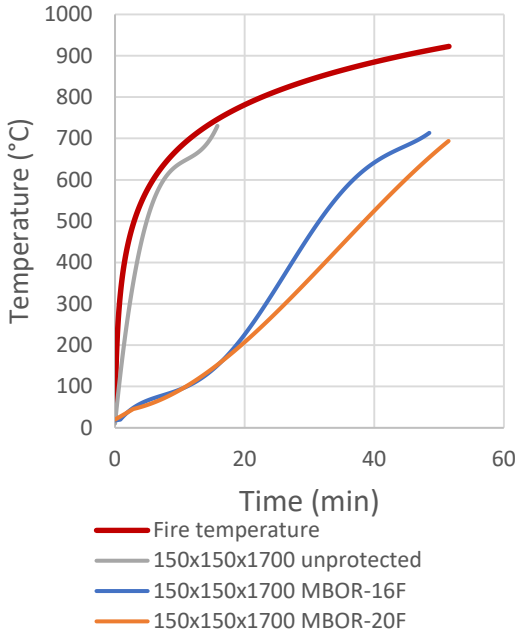

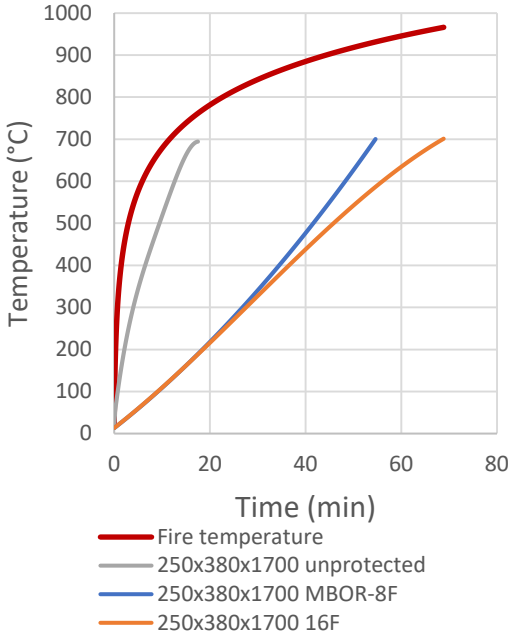

Figure 10. Experimental results for Sample No.1 **Figure 11. Experimental results for Sample No.2**

Based on the results of the fire tests, an approximation of the experimental data is obtained in the form of a mathematical temperature-on-time dependence. In describing the temperature curves, polynomials were chosen as the regression functions. The value of the reliability of the approximation of test results is more than R^2 = 0.99.

Steel sample 1, 150×150×1700 with the reduced metal thickness t_{red1} = 1.01 mm (section factor 990.1 m^{-1}):

$$y = 0.399377 \cdot x^3 - 13.14785 \cdot x^2 + 154.99586 \cdot x + 10.42116$$

Steel sample 2 with the reduced metal thickness t_{red2} = 2.35 mm (section factor 423.7 m^{-1}):

$$y = -0.0155 \cdot x^4 + 0.6078 \cdot x^3 - 9.1114 \cdot x^2 + 94.023 \cdot x + 35.43$$

Based on the obtained approximating functions, a nomogram of heating temperature development of the unprotected steel elements according to the standard fire mode is shown in Fig. 12. Using this figure, the actual fire resistance limit of unprotected steel structures is determined from the loss of bearing capacity in a fire.

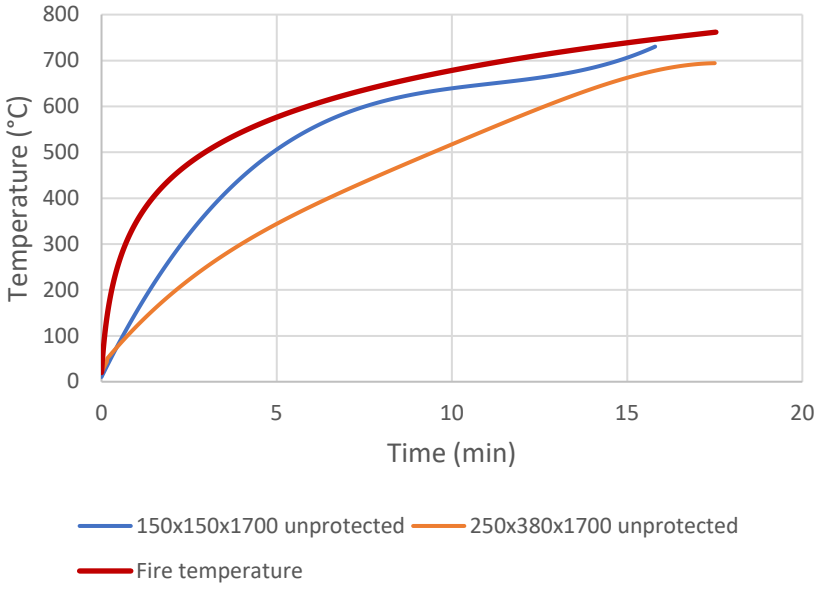

Figure 12. Temperature-time curves of the unprotected elements of steel structures obtained during two full-scale experimental tests according to the standard fire mode (ISO curve).

3.2. Simulation results

Modeling of the temperature distributions of the corresponding sections are based on the data of the fire tests (Figure 13).

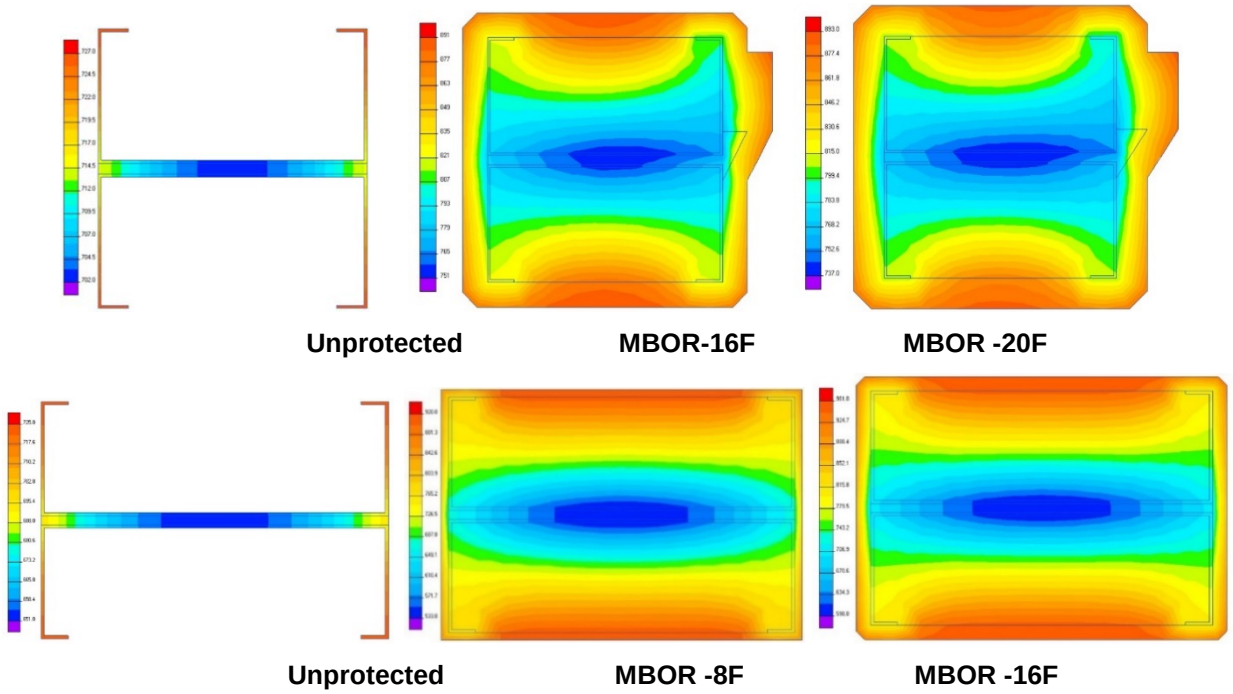

Figure 13. Temperature increase of design samples No. 1 and No. 2.

The simulated temperatures in the middle section of the built-up profile obtained by the fire test method differ from the calculation method in the software package. Moreover, the temperature of the smaller section (sample No. 1) calculated by the theoretical method is greater than the temperature obtained as a result of the experiment. An analysis of the measurement results and error sources for sample No. 2, on the contrary, sets the temperature of the real experiment larger than that calculated in the ELCUT software package. Figure 13 shows the visualization of the section heating in the corresponding measurement scale in the ELCUT software package. The convergences of the FEM to the experimental data for different test conditions are presented in Fig. 14–19.

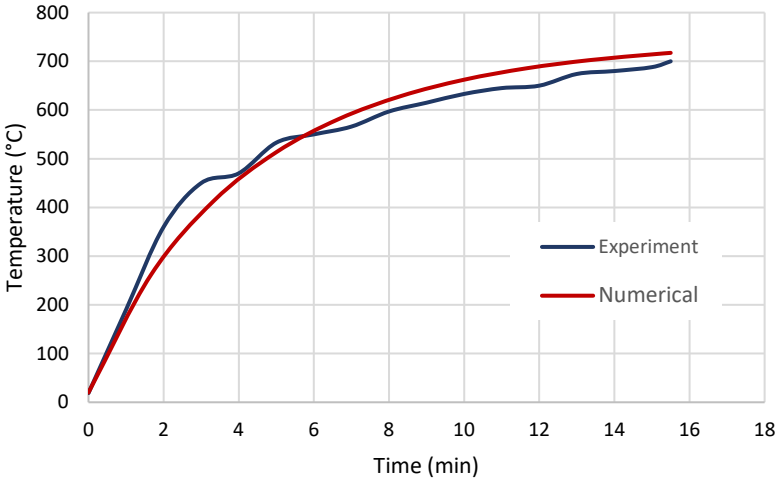

Figure 14. Test 1. First prototype without fire protection.

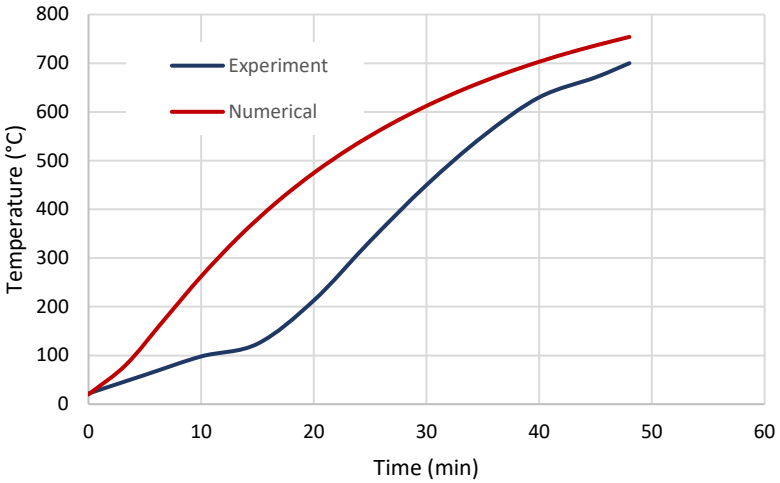

Figure 15. Test 2. First prototype MBOR-16F.

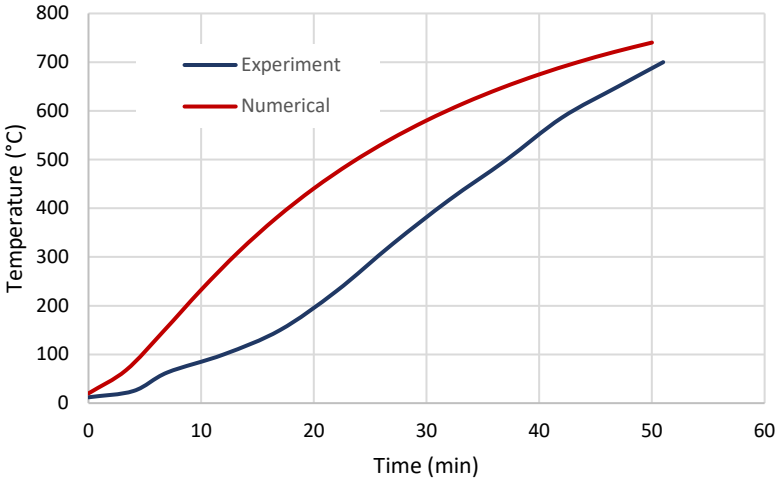

Figure 16. Test 3. First prototype MBOR-20F.

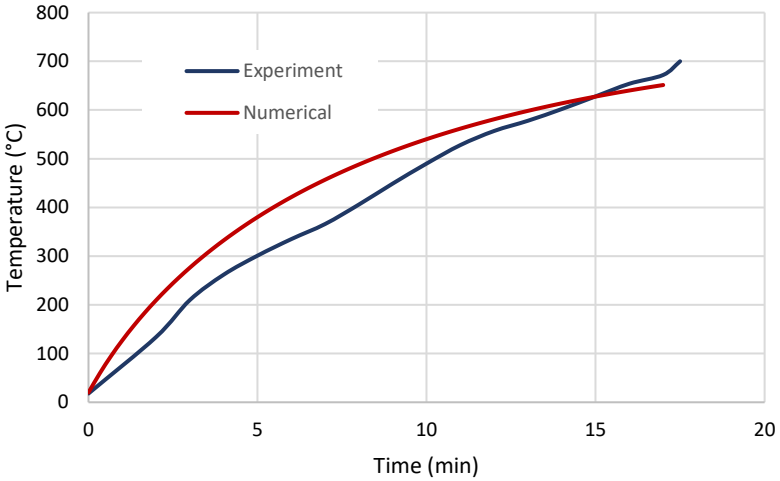

Figure 17. Test 4. Second prototype without fire protection.

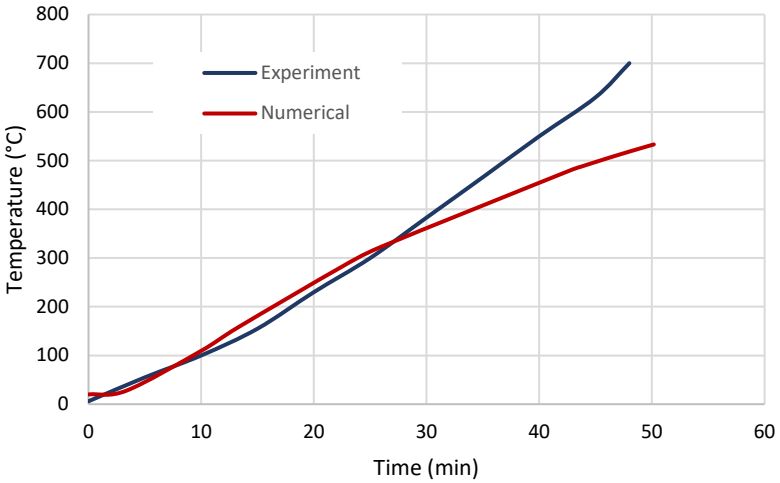

Figure 18. Test 5. Second prototype MBOR-8F.

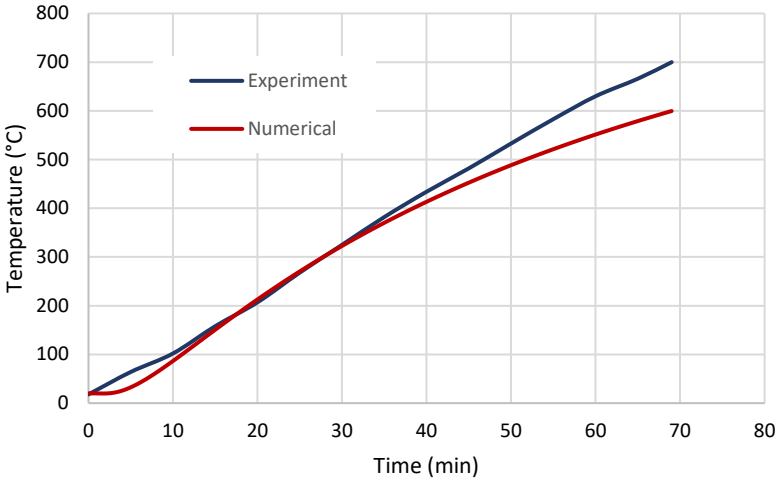

Figure 19. Test 6. Second prototype MBOR-16F.

Fig. 14–19 show the time from the start of a fire test to the achievement of a prototype with a reduced metal thickness of 1.01 mm and that fire protection with MBOR-16F basalt material of the 500 °C critical temperature was 32.5 minutes according to Russian standard No. 53295-2009. A similar sample with MBOR-20F reached its limit state after 37 minutes.

Samples with a reduced metal thickness of 2.35 mm with the coating MBOR-8F reached a critical temperature after 37 minutes, which corresponds to the 6th group of fire-protective efficiency with MBOR-16F fireproof plates in according to Russian standard No. 53295-2009, which reached a critical temperature after 48 minutes.

The simulated temperatures in the middle section of the samples obtained after reaching a given period of time are presented in Table 5. The fire resistance of the structure is evaluated by comparing the results of fire tests based on determining the time to reach the critical temperature of the steel structure with the numerical simulation tests in ELCUT PC. The calculated temperature is obtained in the course of theoretical studies and compared with the results of the standard fire tests.

The Q value taken as the deviation of the obtained temperature T_{pr} in the ELCUT PC from the critical temperature T_{cr}, calculated by formula (5), is determined in percentage by the formula:

$$Q = \left(\left(T_{pr} - T_{cr} \right) / T_{cr} \right) \cdot 100\%, \tag{5}$$

where T_{cr} is a critical temperature, °C;

T_{pr} is a simulation temperature, °C;

Q is a deviation of simulation results from experiment, %.

A table of temperatures obtained and their correlations with the fire tests are presented in Table 3.

Table 3. Temperature correlations with the fire tests.

t_{red}, mm	MBOR -F	T_{pr}, °C	T_{cr}, °C	Time (min)	Q, %
1.01	–	717.34	700	15	2.5
	16	752.0		48	7.4
	20	737.8		50	5.4
2.35	–	651.31	700	17	-7.0
	8	522.7		50	-25.3
	16	599.7		69	-14.3

The data presented in Table 3 shows that the best convergence of the simulated temperature with the actual results of fire tests with the difference up to 7.4 % was shown in the calculations of sample No. 1. The design temperature of an unprotected structure for sample No. 2 differs by less than 10 % with fire tests and by 25.3 % and 14.3 % with using MBOR-8F and MBOR-16F fire protection means respectively.

4. Conclusions

1. The numerical simulations in the ELCUT PC of light steel thin-walled C-profile structures without fire protection and with fire protection of MBOR-F basalt roll material and PLAZAS adhesive composition manufactured by TIZOL JSC showed good agreements with the experimental data (less than 10 %) obtained in the testing laboratory JSC "TIZOL". Some deviations of the simulation results are possibly associated with insufficient data on the thermophysical characteristics of the materials under study.

2. Experimental studies of the fire resistance limits of LGSC structures were analyzed in accordance with the fire-protective efficiency. The values of fire-protective efficiency for the steel rods of a C-shaped profile without fire protection and with the use of MBOR-F basalt wool 8, 16 and 20 mm thickness were obtained.

3. The approximating functions on the basis of the fire test program were formed. The nomogram for heating the steel structure was constructed based on this data. There was no deformation of the samples and destruction of the fire-protective material in the heated surface during the fire tests. The fire-protective efficiency of the LGSC was increased by 2 to 4 times. The numerical simulation results correlated well with the experimental studies, which allows for the predicting of the necessary characteristics of materials and the optimization of the costs of their development and fire tests.

References

1. Zhmarin, E.N. International association of light-gauge steel construction. Construction of Unique Buildings and Structures. 2012. 2(2). Pp. 27–30. (Russian)

2. Construction.RU. All-Russian industry online magazine [Electronic resource]. URL: https://rcmm.ru/tehnika-i-tehnologii.html (date of application: 12.05.2015).
3. Musorina, T.A., Gamayunova, O.S., Petrichenko, M.R., Soloveva, E. Boundary layer of the wall temperature field. Advances in Intelligent Systems and Computing. 2020. Vol. 1116. pp. 429-437. DOI: 10.1007/978-3-030-37919-3_42
4. Musorina, T., Gamayunova, O., Petrichenko, M. Thermal regime of enclosing structures in high-rise buildings. Vestnik MGSU. 2018. Vol. 13. Pp. 935–943.
5. Terekh, M., Tretyakova, D. Primary energy consumption for insulating. E3S Web of Conferences. 2020. Vol. 157. Pp. 1–8 [Electronic resource]. DOI: 10.1051/e3sconf/202015706008
6. Zemitis, J., Terekh, M. Optimization of the level of thermal insulation of enclosing structures of civil buildings. MATEC Web of Conferences. 2018. Vol. 245(68): 06002. DOI: 10.1051/matecconf/201824506002
7. Vatin, N. et al. Simulation of cold-formed steel beams in global and distortional buckling. Applied Mechanics and Materials. 2014. Vol. 633–634. Pp. 1037–1041. DOI: 10.4028/www.scientific.net/AMM.633-634.1037
8. Garifullin, M., Nackenhorst, U. Computational analysis of cold-formed steel columns with initial imperfections. Procedia Engineering. 2015. Vol. 117. No. 1. P. 1073–1079.
9. Garifullin, M. et al. Buckling analysis of cold-formed c-shaped columns with new type of perforation. Advances and Trends in Engineering Sciences and Technologies - Proceedings of the International Conference on Engineering Sciences and Technologies, ESaT 2015. 2016. Pp. 63–68. DOI: 10.1016/j.proeng.2015.08.239
10. Garifullin, M.R., Vatin, N.I. Buckling analysis of thin-walled cold-formed beams — short review. Construction of Unique Buildings and Structures. 2014. No. 6(21). 2014. Pp. 32–57. (rus)
11. Vatin, N.I., Popova, Ye.N. Termoprofil v legkikh stalnykh stroitelnykh konstruktsiyakh [Thermoprofile in light steel building structures] SPb.: Izd-vo SPbGPU, 2006. 63 p. (rus)
12. Gravit, M.V. et al. Software packages for calculation of fire resistance of building construction, including fire protection. IOP Conference Series: Materials Science and Engineering. 2018. Vol. 456. No. 1. DOI: 10.1088/1757-899X/456/1/012016
13. Gravit, M., Dmitriev, I., Lazarev, Y. Validation of the Temperature Gradient Simulation in Steel Structures in SOFiSTiK. Advances in Intelligent Systems and Computing. 2019. Vol. 983. Pp. 929–938. DOI: 10.1007/978-3-030-19868-8_92
14. Gravit, M.V., Nedryshkin, O.V. Full-scale tests for the simulation of fire hazards in the building with an atrium. Advances and Trends in Engineering Sciences and Technologies III- Proceedings of the 3rd International Conference on Engineering Sciences and Technologies, ESaT 2018. 2019. P. 375–380.
15. Gravit, M.V., Golub, E.V., Antonov, S.P. Fire protective dry plaster composition for structures in hydrocarbon fire. Magazine of Civil Engineering. 2018. 79(3). Pp. 86–94. DOI: 10.18720/MCE.79.9
16. Naser, M.Z., Degtyareva, N.V. Temperature-induced instability in cold-formed steel beams with slotted webs subject to shear. Thin-Walled Struct. 2019. Vol. 136. Pp. 333–352. DOI: 10.1016/j.tws.2018.12.030
17. Naser, M.Z., Uppala, V.A. Properties and material models for construction materials post exposure to elevated temperatures. Mech. Mater. 2020. Vol. 142. DOI: 10.1016/j.mechmat.2019.10329318
18. Zhou, H. et al. Behavior of prestressed stayed steel columns under fire conditions. Int. J. Steel Struct. 2017. Vol. 17. No. 1. Pp. 195–204. DOI: 10.1007/s13296-015-0074-4
19. Chen, W. et al. Full-scale experiments of gypsum-sheathed cavity-insulated cold-formed steel walls under different fire conditions. J. Constr. Steel Res. 2020. Vol. 164. P. 105809. DOI: 10.1016/J.JCSR.2019.105809
20. Chen, W., Ye, J., Zhao, Q. Thermal performance of non-load-bearing cold-formed steel walls under different design fire conditions. Thin-Walled Struct. 2019. Vol. 143. P. 106242. DOI: 10.1016/J.TWS.2019.106242
21. Chen, W., Ye, J., Li, X. Fire experiments of cold-formed steel non-load-bearing composite assemblies lined with different boards. J. Constr. Steel Res. 2019. Vol. 158. Pp. 290–305. DOI: 10.1016/j.jcsr.2019.04.003
22. Chen, W., Ye, J., Li, X. Thermal behavior of gypsum-sheathed cold-formed steel composite assemblies under fire conditions. J. Constr. Steel Res. 2018. Vol. 149. Pp. 165–179. DOI: 10.1016/j.jcsr.2018.07.023
23. Chen, W. et al. Improved fire resistant performance of load bearing cold-formed steel interior and exterior wall systems. Thin-Walled Struct. 2013. Vol. 73. Pp. 145–157. DOI: 10.1016/J.TWS.2013.07.017
24. Dias, Y., Keerthan, P., Mahendran, M. Fire performance of steel and plasterboard sheathed non-load bearing LSF walls. Fire Saf. J. 2019. Vol. 103. Pp. 1–18. DOI: 10.1016/J.FIRESAF.2018.11.005
25. Dias, Y., Mahendran, M., Poologanathan, K. Full-scale fire resistance tests of steel and plasterboard sheathed web-stiffened stud walls. Thin-Walled Struct. 2019. Vol. 137. P. 81–93. DOI: 10.1016/j.tws.2018.12.027
26. Craveiro, H. Fire resistance of cold-formed steel columns. Universidade de Coimbra. 2015. P. 366.
27. Agafonova, V.V. Computational modeling during assessment of fire resistance of steel constructions with the use vermiculite fire protection. Izvestiya SFedU. Engineering Sciences. 2013. Pp. 173–177.
28. Golovanov, V.I., Pavlov, V.V., Pekhotikov, A.V. Fire protection of steel structures with slab material PYRO-SAFE AESTUVER T. Fire and explosion safety. 2016. Vol. 125. Pp. 8–15. DOI: 10.18322/PVB.2016.25.11.8-16
29. Gernay, T. Book Review: Fire Performance of Thin-Walled Steel Structures by Yong Wang, Mahen Mahendran, and Ashkan Shahbazian. Fire Technol. 2021. 57. Pp. 973–975 . https://doi.org/10.1007/s10694-020-01082-x
30. Seo, J.K., Lee, S.E., Park, J.S. A method for determining fire accidental loads and its application to thermal response analysis for optimal design of offshore thin-walled structures. Fire Safety Journal. 2017. Vol. 92. Pp. 107–121. https://doi.org/10.1016/j.firesaf.2017.05.022
31. Shahbazian, A., Wang, Y.-C. A fire resistance design method for thin-walled steel studs in wall panel constructions exposed to parametric fires. Thin-Walled Structures. 2014. Vol. 77. Pp. 67–76 https://doi.org/10.1016/j.tws.2013.12.001
32. Feng, M., Wang, Y.C., Davies, J.M. Thermal performance of cold-formed thin-walled steel panel systems in fire. Fire Safety Journal. 2003. Vol. 38. No. 4. Pp. 365–394. https://doi.org/10.1016/S0379-7112(02)00090-5
33. Feng, M., Wang, Y.C., Davies, J.M. Structural behaviour of cold-formed thin-walled short steel channel columns at elevated temperatures. Part 1: experiments. Thin-Walled Structures. 2003. Vol. 41. No. 6. Pp. 543–570. https://doi.org/10.1016/S0263-8231(03)00002-8

34. Wang, W., Qin, S. Experimental investigation of residual stresses in thin-walled welded H-sections after fire exposure. Thin-Walled Structures. 2016. 101. Pp. 109–119. https://doi.org/10.1016/j.tws.2016.01.005
35. Pyl, L., Schueremans, L., Dierckx, W., Georgieva, I. Fire safety analysis of a 3D frame structure based on a full-scale fire test. Thin-Walled Structures. 2012. Vol. 61. Pp. 204–212. https://doi.org/10.1016/j.tws.2012.03.023
36. Russian standard GOST 53295-2009 «Fire retardant compositions for steel constructions. General requirement. Method for determining fire retardant efficiency»
37. ISO 834-1:1999 Fire-resistance tests — Elements of building construction — Part 1: General requirements
38. Zinevich, L.V. Primenenie chislennogo modelirovaniya pri proektirovanii tekhnologii obogreva i vyderzhivaniya betona monolitnykh konstruktsiy. [The use of numerical modeling in the design of heating technology and concrete curing of monolithic structures]. Magazine of Civil Engineering. 2011. No. 2(20). Pp. 24–28. DOI: 10.18720/MCE.20.5.
39. Pukhkal, V.A., Mottaeva, A.B. FEM modeling of external walls made of autoclaved aerated concrete blocks. Magazine of Civil Engineering. 2018. Vol. 81. No. 5. Pp. 202–211. DOI: 10.18720/MCE.81.20.
40. Nazmeeva, T.V., Vatin, N.I. Numerical investigations of notched C-profile compressed members with initial imperfections. Magazine of Civil Engineering. 2016. Vol. 62. No. 2. Pp. 92–101. DOI: 10.5862/MCE.62.9.
41. Dudin, M.O., Vatin, N.I., Barabanshchikov, Y.G. Modeling a set of concrete strength in the program ELCUT at warming of monolithic structures by wire. Magazine of Civil Engineering. 2015. Vol. 54. No. 2. Pp. 33–45. DOI: 10.5862/MCE.54.4.
42. Organization Standard ADSC 11251254.001-018-03 Design of Fire Protection of Load-Bearing Steel Structures Using Various Types of Linings; Association for the Development of Steel Construction; Axiom Graphics Union: Moscow, Russia, 2018; ISBN 9785604087855.

Information about authors:

Marina Gravit
PhD in Technical Science
ORCID: https://orcid.org/0000-0003-1071-427X
E-mail: marina.gravit@mail.ru

Ivan Dmitriev
ORCID: https://orcid.org/0000-0002-9822-3637
E-mail: i.i.dmitriev@yandex.ru

Received 01.08.2020. Approved after reviewing 07.09.2021. Accepted 02.02.2022.